Basic Design of the Maglev Pump for Total Artificial Heart by using Double Stator Type Axial Self-bearing Motor

Nobuyuki KURITA*, Takeo ISHIKAWA*, Naoki SAITO and Toru MASUZAWA **

*Dev. of Electronics and Informatics, Gunma University

1-5-1 Tenjin, Kiryu, Gunma 376-8515, JAPAN

E-mail: nkurita@gunma-u.ac.jp

**Dept. of Mechanical Eng., Ibaraki University

4-12-1 Nakanarusawa, Hitachi, Ibaraki 316-8511, JAPAN

Abstract

Due to the high rate of heart disease and a shortage of donor hearts, there has been a longstanding interest to develop mechanical replacements for the heart. A magnetically levitated motor is one of the key technology to develop a total artificial heart and bi-ventricular assist device.

A double side stator type axial self-bearing motor with a tilt control function, in addition to rotation and translation motion control, was proposed. A slice rotor can be used due to tilt control function. The surface area of a stator and a rotor becomes large. The high torque self-bearing motor is realizable. The operating principle of the proposed self-bearing motor was explained and fundamental characteristics of the motor were tested. In addition, a basic design of the maglev pump by using the proposed axial SBM is presented.

The operating principle was clarified that rotation control, translation control and tilt control show no interference. These four axes are, therefore, able to be controlled independently. According to the experimental result, the fabricated self-bearing motor showed good levitation and rotation performance. Moreover, the basic design of the maglev pump was presented.

Keywords : Self-bearing motor, double stator type, artificial heart, maglev pump

1. Introduction

Due to the high rate of heart disease and shortage of donor hearts, there has been a longstanding interest to develop mechanical replacements for the heart. Recently, third generation rotary blood pumps of implantable size have shown considerable promise in this application. These devices utilize magnetic bearings to support the impeller that eliminates any mechanical contact. The vast majority of devices developed around the world, provide left ventricular assistance. However, right ventricular heart failure may develop in up to 20% of patients receiving left ventricular assistance (Nobuyuki, 2014). In order to develop a total artificial heart and bi-ventricular assist device, a magnetically levitated motor (maglev motor) is one of the key technology. It can provide can realize the non-contact support and rotation of a rotor by magnetic force. Therefore, it has many advantages over conventional mechanical bearing supported motors (Gerhard, 2009), (Andres, 2000). To down size a maglev motor and to simplify the control system, several types of self-bearing motor (SBM) were proposed and researched. Radial-SBM (Yohji, 1995), (Reto, 1997), (Junichi, 2011) controls two radial directions actively while the remaining three axes are controlled passively. Axial-SBM (Satoshi, 2000), (Masahiro, 2012) controls only one axial direction directly while the remaining four axes are controlled passively. In order to increase passive stability, the rotor shape should be slice or cylindrically long and thin to an active control direction. Because of the stator shape, permanent magnet (PM) size and stator surface area will be decreased. They are associated with low rotation torque and weak active control force.

A double side stator type axial SBM with a tilt control function, in addition to rotation and translation motion control was proposed. A slice rotor can be used due to tilt control function. The surface area of a stator and a rotor becomes large. High torque SBM is realizable. This paper explains the operating principle of the SBM and fundamental characteristics of the motor. In addition, a basic design of the maglev pump by using the axial SBM is presented.

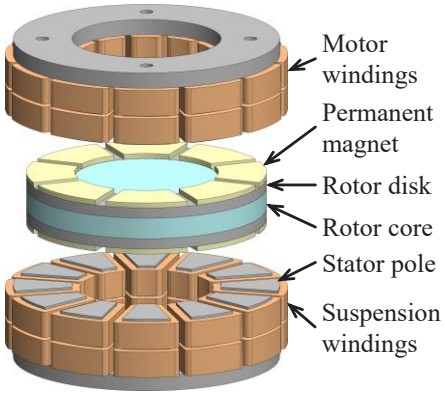

Fig. 1. Schematic of the proposed self-bearing motor

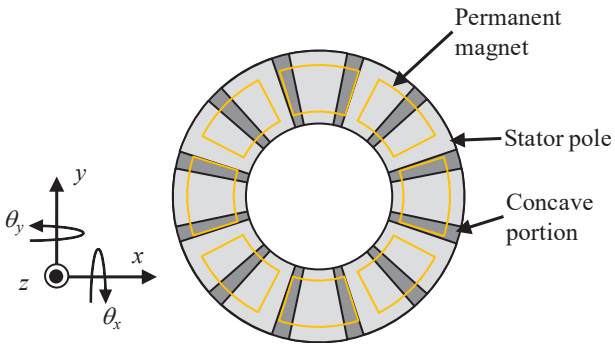

Fig. 2. Layout of permanent magnets and stator poles

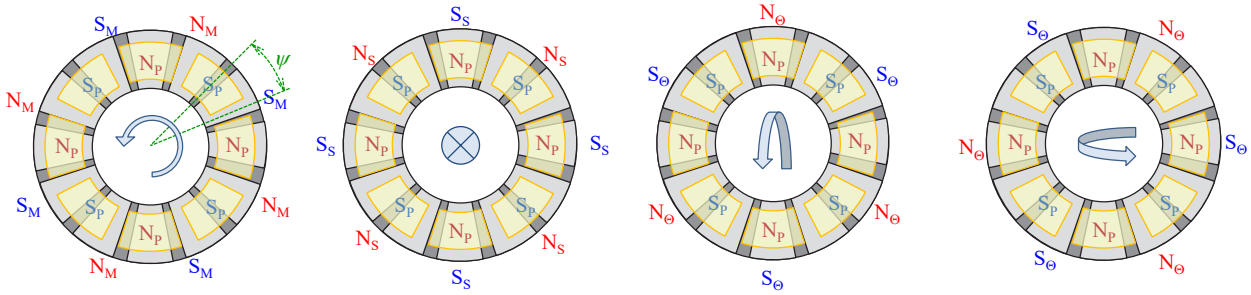

(a) torque control (b) translation control (c) tilt θx control (d) tilt θy control

Fig. 3. Magnetic pole arrangement for levitated rotation control

2. Proposed self-bearing motor

A schematic of the proposed maglev motor is shown in Fig. 1. Eight pole PMs are located on each side of the rotor. The stator has twelve poles. Each stator pole has three-phase eight-pole winding for rotation and axial motion control, and two-phase six-pole windings for tilting motion control. The rotor is installed in the center of two identical stators as shown in the figure. The operation principle of the proposed maglev motor is based on a conventional axial self-bearing motor. The operation principle of the upper side airgap is hereby described. A layout sketch of the PM and stator poles is shown in Fig. 2 and Fig. 3. The figure shows the state that the upper side stator is looked up from the rotor side. The magnetic pole of the PM written in the figure shows the magnetic pole generated at the airgap side. In order to simplify the analysis, a leakage flux and non-linearity of the attractive force are ignored.

The flux density distribution B_{pm} in the airgap produced by the rotor PMs is represented as (1).

$$B_{pm}(\theta,t) = B_P \cos(\omega t - 4\theta) \tag{1}$$

Where, B_P (T) is the maximum flux density of the PM, ω (rad/s) is rotating speed of the rotor, t (sec) is time, θ (rad) is the angle.

In order to generate the rotating torque, eight-pole rotating magnetic field of phase difference ψ (rad) should be generated by the motor current as shown in Fig. 3(a). In addition, in order to control the axial translation motion, eight-pole magnetic field of the same phase of the PM should be generated as shown in Fig. 3(b). Meanwhile, in order to control the tilt motion, six phase magnetic field should be generated shown in Fig. 3(c) and (d). Therefore, the torque control flux density B_m, the axial translation control flux density B_s, and the tilt control flux density $B_{\theta x}$ and $B_{\theta y}$ are represented as (2), respectively.

$$\begin{aligned} B_m(\theta,t) &= B_M \cos(\omega t - 4\theta + \psi), & B_s(\theta,t) &= B_S \cos(\omega t - 4\theta) \\ B_{\theta x}(\theta,t) &= B_\Theta \sin(\omega t - 3\theta), & B_{\theta y}(\theta,t) &= B_\Theta \cos(\omega t - 3\theta) \end{aligned} \tag{2}$$

Where, B_M, B_S and B_Θ is the peak value of the flux density produced by the motor current, the suspension current and the tilt control current, respectively.

Magnetic energy ΔW in the infinitesimal volume of the airgap ΔV is as follows.

$$\Delta W = \frac{B^2}{2\mu_0}\Delta V = \frac{B^2}{2\mu_0}\cdot z\pi(r_o{}^2 - r_i{}^2) \tag{3}$$

Where, μ_0 is the permeability of the vacuum, and r_o and r_i are outer and inner diameter of the stator, respectively.

The rotating torque and the suspension force are derived from partially differentiating magnetic energy ΔW with regard to phase difference ψ and gap length z, respectively. According to (2) and (3), the rotating torque τ_z and the suspension force F_z are as follows.

$$\tau_z = \frac{\partial W_M}{\partial \psi} = \frac{2z\pi(r_o{}^2 - r_i{}^2)}{\mu_0} B_P B_M \sin\psi \tag{4}$$

$$F_z = \frac{\partial W_S}{\partial z} = \frac{\pi(r_o{}^2 - r_i{}^2)}{4\mu_0}\left\{B_P{}^2 + 2B_P B_S \cos\psi + B_S{}^2\right\}$$

The restoring torque is a product of the attractive force by the tilt control current and the distance from the center of the Gravity to point of application of the force. According to (4), the restoring torque τ_x and τ_y are as follows.

$$\tau_x = \frac{\partial W_\theta}{\partial z}\times\frac{r_o + r_i}{2} = \frac{\pi(r_o + r_i)(r_o{}^2 - r_i{}^2)}{16\mu_0}\left\{B_P{}^2 + 2B_P B_\theta \sin\theta + B_\theta{}^2\right\} \tag{5}$$

$$\tau_y = \frac{\pi(r_o + r_i)(r_o{}^2 - r_i{}^2)}{16\mu_0}\left\{B_P{}^2 + 2B_P B_\theta \cos\theta + B_\theta{}^2\right\}$$

According to (4) and (5), motoring torque τ_z is controlled only by motor control flux density B_M. The axial translation control flux density B_s and the tilt control flux density $B_{\theta x}$ and $B_{\theta y}$ are not affect motor torque. Also in other motion control, it turned out that each magnetic flux density does not affect other motion control. It is therefore theoretically apparent that rotating torque, suspension force and restoring torque can be controlled independently.

3. Experimental setup

3.1 Magnetically levitated motor

In order to clarify the operation principle, a simple experimental setup was designed based on FEM (Nobuyuki, 2013) and fabricated. Fig. 4(a) shows a photo of an entire unit of the experimental setup. Stators are fixed to the stator holder. The rotor is placed between upper and lower stator. Although, it is omitted in the figure, three eddy current type displacement sensors were installed to detect translation motion and tilt motion of the rotor, and three hall ICs are installed lower side of the sensor target. Thirty-six small PMs are attached to the sensor target. Hall IC detects those PMs and operates as a rotary encoder. Fig. 4(b) shows a photo of the stator. The stator was made of pressed powder core in order to reduce eddy current loss. Two type of winding are attached to one stator pole, respectively. One type of winding is motor and translation control winding. The other type of winding is tilting control winding. Fig. 4(c) shows a photo of the rotor. The rotor core was made of acrylate resin. An iron disk was attached to the rotor core as a sensor target. Sensor target was made of stain- less steel (SUS304 in Japanese Industrial Standard: JIS). The rotor disk (back-yoke) was made of pure iron (SUY-1: JIS). PMs are made of Nd-Fe-B sintered magnets (N48H: JIS). Sizes of each component are listed in Table I.

Table 1. Sizes of the experimental setup

Rotor	
Rotor disk outer diameter	ϕ45 mm
Rotor disk inner diameter	ϕ27 mm
Rotor disk thickness	2 mm
Sensor target outer diameter	ϕ85 mm
Sensor target thickness	2 mm
PM outer diameter	ϕ45 mm
PM inner diameter	ϕ27 mm
PM thickness	1 mm

Stator	
Stator outer diameter	ϕ50 mm
Stator inner diameter	ϕ27 mm
Stator pole height	13 mm
Stator base height	3 mm
Windings	
Motor and axial winding	100 turns/pole
Tilt winding	50 turns/pole

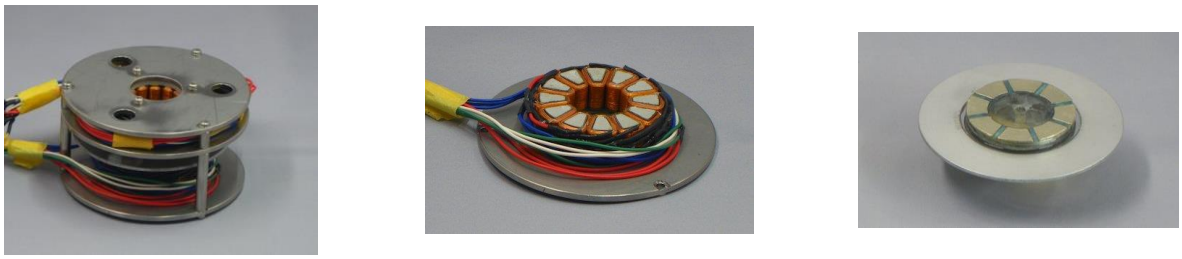

(a) entire unit (b) stator (c) rotor

Fig. 4. Photo of the fabricated experimental setup

3.2 Control system

The rotor displacement z_1, z_2 and z_3 detected by the three sensors (Sensor head: EX-110, sensor amp: EX-202, KEYENCE) are used to calculate axial displacement of the center of the gravity z and the rotor tilts θ_x, θ_y. Calculated displacement signals are fed to a digital signal processor (DSP, dSPACE DS1104) via AD converter. Three independent digital PID controllers for these signals are constructed by the DSP. The PID controllers calculate control current reference values for each axis. The current references are converted to three-phase translation control current reference and two- phase tilt control current reference. The converted current references are input to linear amplifiers. Control current is then fed to each winding from the linear amplifiers. The PID gains were tuned by trial and error method based on the time responses of the rotor. The sampling time interval was $\tau = 0.1$ msec.

4. Experimental results

4.1 Magnetically levitation performance

In order to clarify the levitation control performance, impulse responses were measured. An impulsive disturbance signal was added to the control signal. The experimental results are shown in Fig.5. Translation control gains for levitation control were as follows; proportional gain K_{ZP} = 5.88 A/mm, derivative gain K_{ZD} = 0.0097 A·sec/mm, Integrated gain K_{ZI} = 10.0 A/(mm·sec). Tilt control gains are follows; proportional gain $K_{\theta P}$ = 4.41 A/deg, derivative gain $K_{\theta D}$ = 0.103 A·sec/deg, Integrated gain $K_{\theta I}$ = 10.0 A/(deg·sec).

After adding disturbance impulse signals, the time taken for rotor vibration to reduce below ±5% of the maximum displacement was about 0.023sec for z-direction, about 0.019 sec for tilt directions, respectively. The levitation control therefore demonstrated a good time response.

There was almost no vibration in tilt motion of Fig. 5(a) due to z-direction disturbance. There was very small vibration in z-direction of Fig. 5(b) and (c) due tilt direction disturbance. It is therefore experimentally apparent that suspension force and restoring torque can be controlled independently.

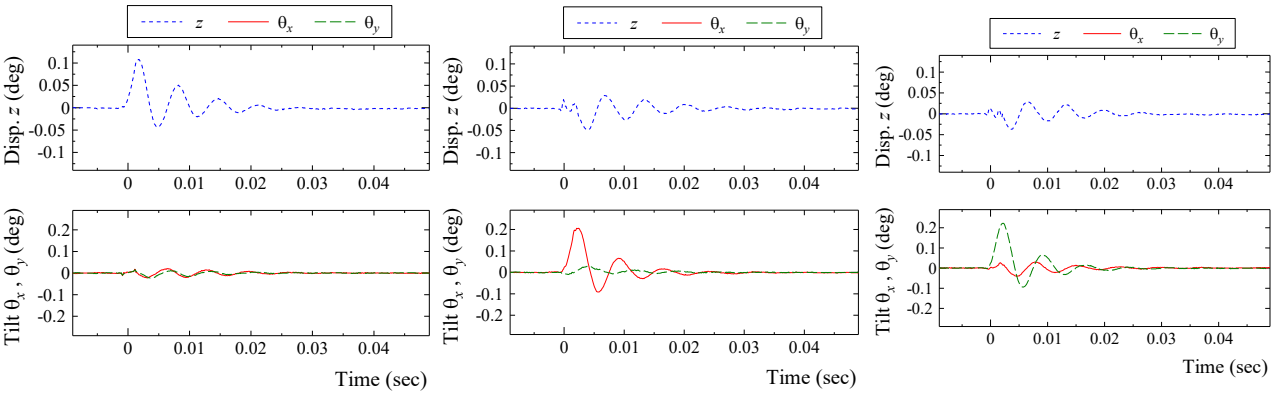

(a) disturbance direction: z-dir. (b) disturbance direction: θ_x-dir. (c) disturbance direction: θ_y-dir.

Fig. 5. Impulse response

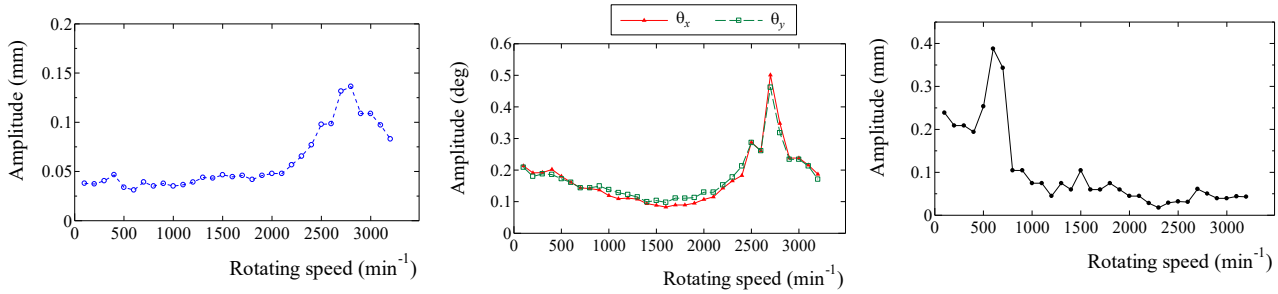

(a) axial translation motion vibration (b) tilt motion vibration (c) radial translation motion vibration

Fig. 6. Vibration amplitude versus rotating speed

4.2 Magnetically levitated rotation performance

In order to confirm levitated rotation characteristics, vibration amplitude for each rotating speed were measured. The experimental results are shown in Fig. 6. Translation control gains for levitated rotation were as follows; proportional gain K_{ZP} = 6.48 A/mm, derivative gain K_{ZD} = 0.0144 A·sec/mm, Integrated gain K_{ZI} = 2.0 A/(mm·sec). Tilt control gains are follows; proportional gain $K_{\theta P}$ = 2.5 A/deg, derivative gain $K_{\theta D}$ = 0.0188 A·sec/deg, Integrated gain $K_{\theta I}$ = 2.0 A/(deg·sec). According to the result, a maximum rotating speed of about 3,200 min^{-1} was observed. Maximum vibration amplitude of 0.14 mm at 2,800 min^{-1} in axial direction, 0.5 deg at 2,700 min^{-1} in tilt direction and 0.4 mm at 600 min^{-1} in radial direction were observed, respectively. Large vibration amplitude is considered to be due to the resonance in the rigid body vibration mode. However, the amplitude was sufficiently small. Moreover, stable rotation was achieved above and below the critical speed. Since the radial direction was passive control, resonance frequency existed in the low frequency. In addition, as compared with the activity controlled axis, vibration amplitude was large.

5 Maglev pump design

By using the proposed axial SBM, a maglev pump for TAH application was designed. Fig. 7 shows a schematic of the designed pump. Eight PMs are attached on the rotor back yoke, and the sensor target was arranged around the PMs. Two rotor yokes are connected by a shaft. Impellers for the upper and lower pump are installed on the rotor disks. The shaft is surrounded by a partition plate in order to separate upper flow and lower flow in the pump casing.

Fig. 8 shows an outline of the flow path of the proposed maglev pump. Two rotor yokes are connected by the shaft. PMs are installed on the side of the rotor yokes nearest the stators, while the impeller blades are installed in the inside toward the partition plate. The rotor yoke has a several holes so that fluid can pass through. The stators are installed at the outside of the housing. The stator windings produce the required flux density distribution to control the rotor rotation, axial translation and tilts. Liquid enters the pump at the inlet and passes through the holes of the rotor yoke. The impeller accelerates the fluid towards the outlet by centrifugal force. The flow path between the upper and lower inlet is divided with a partition plate, but some mixing of the two streams does occur.

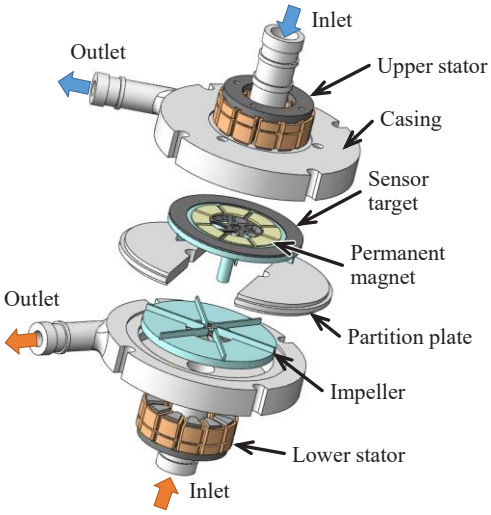

Fig. 7. Schematic of the proposed self-bearing motor

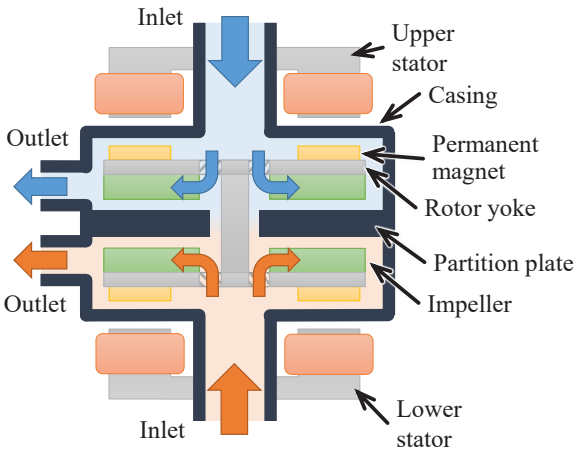

Fig. 8. Layout of permanent magnets and stator poles

6. Conclusion and Future work

A double-sided stator type axial SBM with a tilt, rotational, and translational motion control was proposed, and its operating principle was clarified. Rotation control, translation control and tilt control show no interference. These four axes are therefore, able to be controlled independently. Moreover, the simple experimental setup was fabricated in order to confirm the operating principle and to clarify the levitation and rotation control performance. According to the result, the settled time was 0.023 sec for translation and 0.019 sec for tilt. And the rotation speed of 3,200 min^{-1} was obtained without any serious problem. It is therefore experimentally apparent that the experimental setup has good levitation and rotation performance.

Moreover, the basic design of the maglev pump was presented. An experimental setup of the maglev pump is now being manufactured.

References

Andres O. Salazar, Akira Chiba and Tadashi Fukao, “A Review of Developments in Bearingless Motors”, The proceedings of the Seventh International Symposium on Magnetic Bearings, (2000), pp.335-340

Gerhard Schweitzer, Eric H. Maslen, Magnetic Bearings -Theory, Design, and Application to Rotating Machinery- (2009), Springer.

Junichi Asama, Tetsuro Asami, Takashi Imakawa, Akira Chiba, Atsushi Nakajima, Rahman M. Azizur, “Effects of Permanent-Magnet Passive-Magnetic-Bearing on a 2-axis Actively Regulated Low-Speed Bearingless Motor”, IEEE Transactions on Energy Conversion. 26(1), p. 46-54 (2011)

Masahiro Osa, Toru Masuzawa, Eisuke Tatsumi, “Miniaturized Axial Gap Maglev Motor with Vector Control for Pediatric Artificial Heart”, Journal of JSAEM, Vol. 20, No. 2, pp. 397-403, (2012)

Nobuyuki Kurita, Takeo Ishikawa, “A Study on a Double Stator Type Axial Magnetically Levitated Motor”, 2013 IEEE International Symposium on Industrial Electronics, Paper No. TF-005177, Taipei, Taiwan (2013)

Nobuyuki Kurita, Daniel Timms, Nicholas Greatrex, Matthias Kleinheyer, Toru Masuzawa, “Optimization design of magnetically suspended system for the BiVACOR total artificial heart”, *Proc. of ISMB14*, 437-440 (2014)

Reto SCHOEB, Natale BARLETTA “Principle and Application of a Bearingless Slice Motor”, JSME International Journal Series C, Vol.40, No.4 (1997)

Satoshi Ueno, Yohji Okada, “Characteristics and control of a bidirectional axial gap combined motor-bearing”, IEEE/ASME Transactions on Mechatronics, Vol. 5, Issue 3 (2000), pp. 310-318.

Yohji OKADA, Tetsuo OHISHI, Kazutada DEJIMA “General Solution of Levitation Control of a Permanent Magnet(PM)-Type Rotating Motor”, JSME International Journal Series C, Vol.38, No.3 (1995)